Design and Evaluation of Miniature Control Surface Actuation Systems for Aeroelastic Models

Gerald E. Bergmann* and Francis D. Sevart†
The Boeing Company, Wichita, Kans.

Miniature control surface actuation systems with wide bandpass performance have been developed for two airplane aeroelastic wind tunnel models. Analysis, design, and test results are presented for: 1) electromechanical systems for the elevator, aileron, canard, and flaperon control surfaces of a 1/30 scale B-52 model, and 2) electrohydraulic systems for the trailing edge and leading edge aileron control surfaces of a 1/17 scale semispan delta wing model. The electromechanical systems utilize d.c. torque motors with position and rate feedback to achieve a bandpass capability of 50 Hz. A rotary vane hydraulic actuator (weighing less than 3 oz) and servovalve compensated with position and load pressure feedback have demonstrated a bandpass performance of over 100 Hz.

Introduction

IN 1968 the NASA-Langley Research Center Aeroelasticity Branch procured an aeroelastic model of a B-52E airplane (Fig. 1) and initiated a research program to demonstrate active control of the model's symmetric gust response. Since 1970 Boeing-Wichita has provided technical support to the current NASA-Langley research program directed toward demonstration of active ride control, maneuver load control, and augmented stability systems on the B-52 model and an active flutter suppression system on a NASA SST delta wing semispan model (Fig. 2).[1,2] In June 1972 the Air Force Flight Dynamics Laboratory awarded Boeing-Wichita a research study to obtain wind tunnel data on the NASA B-52 model with an active flutter suppression system for correlation with flight test results from the AFFDL CCV program.

Model modifications were conducted at Boeing-Wichita to add forward body horizontal canards, single segment flaperons, three segment flaperons, outboard ailerons, and associated actuation systems on the B-52 model, and actuation systems for leading edge and trailing edge control surfaces on the delta wing model. During the past two years electromechanical and electrohydraulic control surface actuation systems have been developed for these models. Laboratory and preliminary wind tunnel test results indicate that minature actuation systems can provide satisfactory performance for aeroelastic models with active control systems.

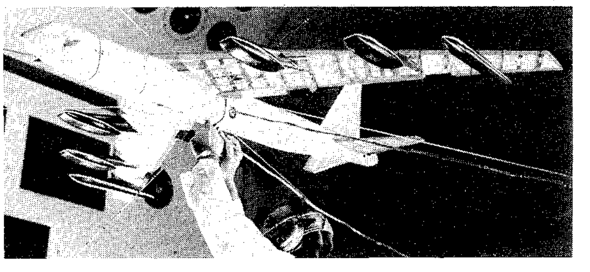

Fig. 1 NASA B-52 aeroelastic model.

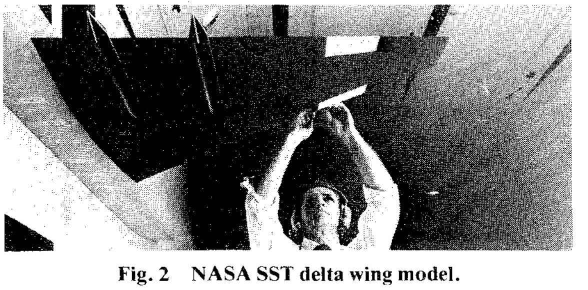

Fig. 2 NASA SST delta wing model.

B-52 Aeroelastic Model Actuation Systems

The one-thirtieth scale B-52 model was built in 1968 with electromechanical actuation systems for the model elevator and ailerons. The control surfaces were to be used for an active gust alleviation system originally planned for demonstration in the Langley Transonic Dynamics Tunnel. Model roll and pitch trim was provided by differential aileron deflections and a d.c. gear reduction motor driving the horizontal stabilizer through a jackscrew arrangement.

The aileron and elevator actuation systems consisted of permanent magnet, brushless d.c. torque motors, and film type rotary potentiometers to provide both torque motor and control surface angular positions. Necessary linkage to drive the surfaces was installed, utilizing oil-less bronze bushings at shaft supports and stainless steel bellows couplings to isolate the shafting from model structure.

Plans for this model were subsequently expanded to include wind tunnel demonstrations of other advanced control systems, such as ride control, flutter suppression, augmented stability, and maneuver load control. Actuation system performance criteria were established for the existing aileron and elevator, and for new inboard single and three segment wing flaperons, outboard wing ailerons, and forward body horizontal canards (Fig. 3). Analytical studies were conducted to determine components required to achieve the desired performance. Mechanization difficulties were identified and solved through testing of breadboard actuation systems.

Design Requirements

The B-52 aeroelastic model mass and stiffness properties were selected to provide aeroelastic characteristics equivalent to the full-scale airplane up to 4.5 Hz, which includes the first

Presented as Paper 73-323 at the AIAA/ASME/SAE 14th Structures, Structural Dynamics and Materials Conference, Williamsburg, Va., March 20-22, 1973; submitted September 7, 1973; revision received October 4, 1974. This research was supported in part by the NASA, Langley Research Center, Contract NAS1-10885.

Index categories: Aeroelasticity and Hydroelasticity; Aircraft Testing (including Component Wind Tunnel Testing); Aircraft Subsystem Design.

*Group Engineer, Flight Controls Research.

†Specialist Engineer, Flight Controls Research.

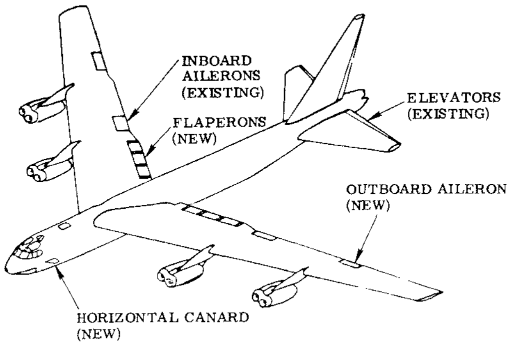

Fig. 3 B-52 aeroelastic model control surface locations.

eight symmetric structural modes. The frequency scale of the Froude Number scaled model is 5.48, resulting in a model frequency range of 0 to 25 Hz.

Control surface actuation system performance requirements were scaled from the B-52 LAMS test airplane (AF56-632) elevator and aileron actuation system performance within this frequency range. The primary objective was to ensure adequate dynamic performance to control elastic modes up to 25 Hz while maintaining sufficient control authority for rigid body motions. Performance and stability requirements are summarized: 1) System frequency response shall not exceed 3 db attenuation and 45° phase lag at 25 Hz for 3° amplitude sinusoidal input command. 2) The motor-load resonance (dominant second order) shall have a nominal damping ratio of 0.3 and a minimum of 0.15. 3) Each control surface actuation system shall be capable of producing at least 6° amplitude up to 20 Hz without power amplifier saturation. 4) Deflection capability, measured at the control surface, must be at least ± 25°. Peak torque at ±19° shall be at least 25 oz-in. for all but the canard torque motor, which shall be at least 5 oz-in. 5) Control surface hysteresis shall not exceed ±0.20°. 6) Control surface-shaft resonance frequency shall be greater than 90 Hz.

The first two requirements translate into a dominant mode with 0.3 damping at an undamped natural frequency of about 250 rad/sec. The torque motors originally installed in the model produce 30 oz-in. peak torque and more than 25 oz.in. at ±19° rotation. With four pole permanent magnets, the motors are capable of ± 30° operation with nominal 0.30 oz-in. maximum residual magnetism. The control surface-shaft resonance frequency requirement dictates that surface inertias be minimized. Friction at all bearing supports must also be minimized to satisfy the hysteresis requirement.

Actuation System Design

Design of the model actuation systems was accomplished through conventional linear analysis to define the components required to meet the desired performance. Representative actuation systems were breadboarded using actual hardware and thoroughly tested to verify the predicted performance.

Analysis

A linearized mathematical model was derived from the simplified motor-load representation shown in Fig. 4. Data from manufacturer's specifications for the torque motors and power amplifiers, and estimates of control surface inertias and shaft stiffness were used to obtain open loop transfer functions of each actuation system for conventional root locus and frequency response system synthesis studies.

The representative root locus shown in Fig. 5 illustrates the need for rate and position feedback to satisfy response and stability requirements. A simplified block diagram of the actuation systems is shown in Fig. 6. Motor shaft position and rate are fed back through constant gain through the power amplifier to the torque motor. Exact feedback gains were

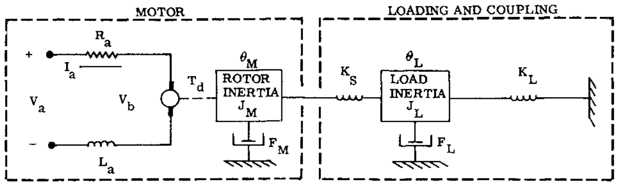

TRANSFER FUNCTIONS:

$$\frac{\theta_M}{V_a}(S) = \frac{K_T\left[J_L S^2 + F_L S + \left(K_S + K_L\right)\right]}{\left[\left(J_M S^2 + F_M S + K_S\right)\left(\tau_a S + 1\right) + DS\right]\left[J_L S^2 + F_L S + \left(K_S + K_L\right)\right] - K_S^2\left(\tau_a S + 1\right)}$$

$$\frac{\theta_L}{\theta_M}(S) = \frac{K_S}{J_L S^2 + F_L S + \left(K_S + K_L\right)}$$

Baseline System $K_S \approx \infty$, $K_L = 0$, $F_L = 0$, $F_M = 0$

$$\frac{\theta_M}{V_a}(S) = \frac{K_T/\tau_a\left(J_M + J_L\right)}{S\left[S^2 + \dfrac{S}{\tau_a} + \dfrac{D}{\tau_a\left(J_M + J_L\right)}\right]} \quad \text{and} \quad \frac{\theta_L}{\theta_M} = 1$$

Fig. 4 Mathematical model of motor and load.

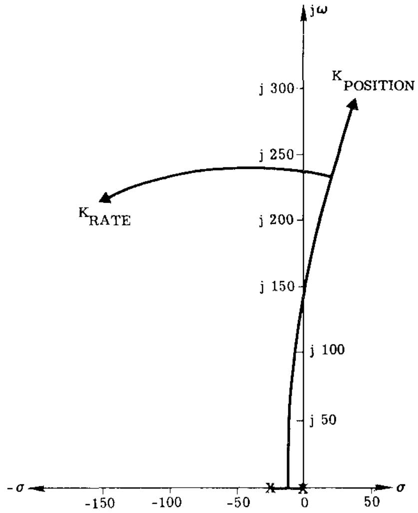

Fig. 5 Typical root locus.

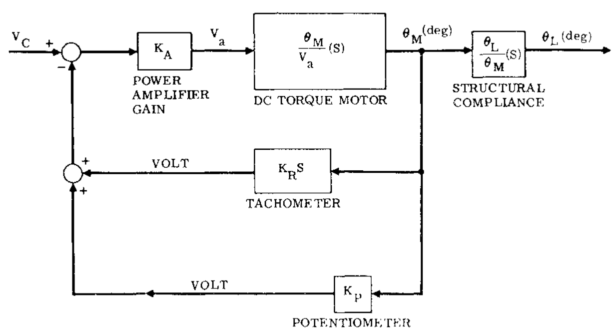

Fig. 6 Simplified block diagram of actuation systems.

determined through laboratory testing of the systems installed in the model. Testing was conducted on breadboard systems to verify the mathematical model and to identify system mechanization problem areas.

Breadboard testing

A breadboard mockup of the model aileron system was mechanized as shown in Fig. 7, using a torque motor from the model. Approximate shaft routing required in the model was included. A wing plate, designed and fabricated to simulate the wing vertical stiffness, permitted evaluation of the system performance with wing flexure similar to that expected during the wind tunnel tests. Figure 8 shows a similar breadboard of

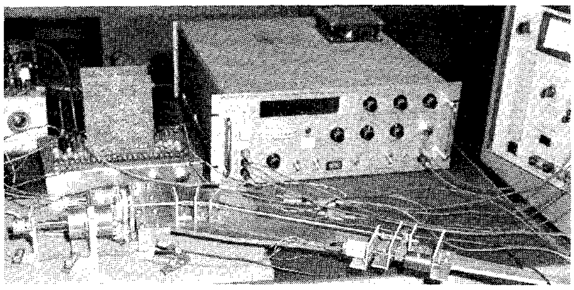

Fig. 7 B-52 model aileron actuation system breadboard.

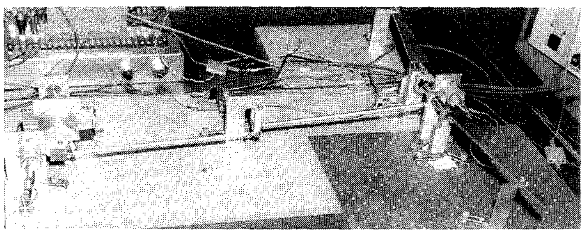

Fig. 8 B-52 model elevator actuation system breadboard.

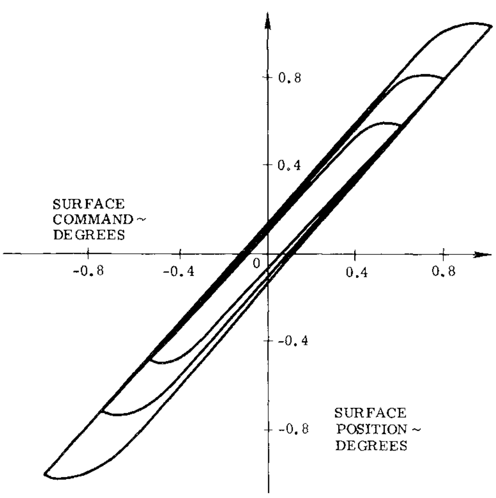

Fig. 9 Aileron actuation system hysteresis.

the elevator system. Rotary induction potentiometers at the motor and control surface were used to evaluate bearing friction and torque motor residual magnestism.

Solutions to primary mechanization problems are summarized below: 1) To meet the hysteresis requirement, precision ball bearings are required at all shaft supports to minimize coulomb friction. The hysteresis of the aileron actuation system using ball bearings is shown in Fig. 9. 2) Stainless steel bellows couplings are superior to universal joints in accomplishing 30° change of direction in shafting. 3) The stainless steel bellows couplings required to decouple shaft stiffness from wing stiffness produce axial and transverse, as well as torsional, vibration modes in the shafting. Thus, couplings with stiffness values as high as possible must be selected to keep these mode frequencies high. 4) Inertia of the original elevator pushrod linkage was excessive. The solid aluminum pushrods were replaced with tubing and the effective crank radius reduced from 0.75 in. to 0.50 in. to meet the required dynamic performance.

Figure 10 shows a comparison of the measured and theoretical frequency responses of a baseline system breadboard, with the simulated load inertia directly coupled with the torque motor. These responses include dynamic effects of a full wave, pulse sampled demodulator used with the in-

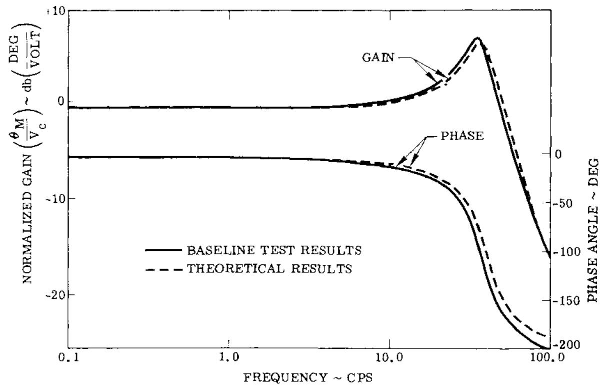

Fig. 10 Comparison of actual and theoretical frequency responses of baseline system.

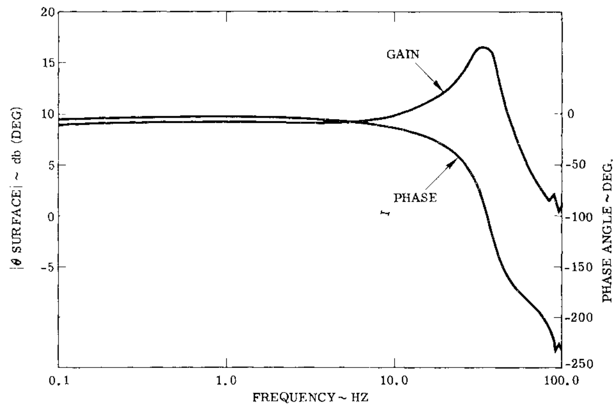

Fig. 11 Aileron actuation system frequency response.

duction potentiometers. Most of the difference between the two responses can be attributed to failure to match with a linear transfer function gain and phase characteristics of the measured demodulator frequency response.

A measured frequency response of the breadboard aileron actuation system is shown in Fig. 11. The response indicates the motor-load mode has about 0.3 damping and an undamped natural frequency of about 39 Hz. The lowest frequency shaft mode occurs at about 90 Hz, but no attempt was made to determine the frequency exactly because of excessive system wear at the high frequencies.

Model Modification

Figure 12 is a photograph of the model with the canard, flaperons, outboard ailerons, and elevator installed. New wing segments were fabricated with the original aileron set in

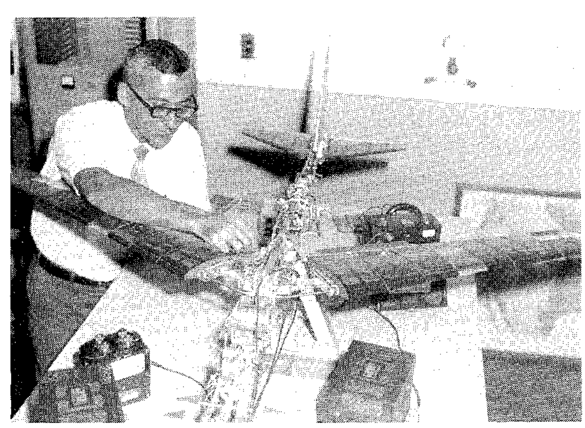

Fig. 12 B-52 aeroelastic model with control systems installed.

the zero position to permit usage of its linkage for the new outboard ailerons. The photograph shows the full three segment flaperons installed in the model. Components were designed and fabricated to permit mechanization of the outboard segments only as required for the flutter suppression system.

All torque motors are installed in the model fuselage with torque transmitted to the control surfaces through crank-pushrod linkage and shafting. Assembly of the linkage requires considerable precision to minimize friction. Final system operating gains and performance will be established just prior to wind tunnel entry.

SST Wing Model Acutation Systems

The NASA one-seventeenth scale supersonic transport wing model consists of a machined aluminum alloy plate covered with balsawood contoured to the airfoil shape. This model was designed and built to represent the flutter characteristics of the Boeing full-scale SST airplane wing design.

The NASA-developed flutter suppression system was formulated using ideal actuators driving model leading and trailing edge ailerons. Realistic performance requirements were established through evaluation of the system performance with nonideal actuator characteristics and hinge moment estimates supplied by NASA. Electrohydraulic actuation of the control surfaces was required to meet the desired performance. Single vane rotary actuators were designed and fabricated specifically for this model and tested extensively with high response servovalves. The model was modified to add the actuation systems and subsequent wind tunnel testing of this model indicates actuation system performance meets or exceeds the desired performance.

Design Requirements

Actuation system performance requirements were established to be as ideal as possible because the flutter suppression system was formulated on the basis of ideal actuation characteristics. The flutter mode frequency is approximately 12 Hz. Hinge moment estimates indicated a maximum torque generation capability of at least 20 lb-in. was required from an actuator mounted at the inboard edge of each control surface where wing thickness is only 0.375 in. at the leading edge surface hinge line and 0.47 in. at the trailing edge surface. The combination of high bandpass and high torque in a small package could only be satisfied with subminiature electrohydraulic actuators.

Performance requirements established for the two actuation systems are summarized as follows: 1) The actuation systems shall have minimum phase and gain variations in the frequency range 5 to 25 Hz. Maximum phase lag at 12 Hz shall not exceed 20°. 2) Maximum control surface deflection shall be at least ±10°. 3) Maximum torque capability shall be at least 20 lb-in. 4) Control surface hysteresis shall not exceed ±0.10°. 5) The actuation system shall not violate the wing airfoil shape.

Actuation System Design

Single vane rotary actuators were designed for installation within the airfoil to produce a maximum torque of 40 lb-in. operating with a 1000 psi supply pressure. Two stage, high performance flow control servovalves were selected to drive the actuators. The actuators were fabricated and a breadboard baseline system assembled and tested to determine problem areas before installation in the model.

Actuator design

A disassembled actuator is shown in Fig. 13. The vane radius and length are nominally 0.50 in. producing a torque constant of 0.0615 lb-in./psi. The stainless steel vane is coated with adiprene to provide sealing between the vane and the actuator body and end caps. The double-ended shaft was fabricated from high strength stainless steel. The shaft was slotted to mate with the vane and spot welded on assembly. The shaft is supported by two 1/8-in. bore precision ball bearings and sealed with O-rings.

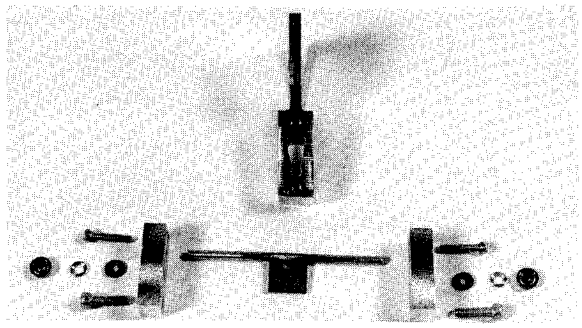

Fig. 13 Subminiature rotary actuator.

Actuator body and end caps were machined from 2024-T4 aluminum plate. Copper wire, 0.0003 in. in diameter, was used as a gasket seal between the actuator body and the two end caps. Miniature elbow fittings were machined from 4340 steel to provide an O-ring seal at the actuator ports located in the end caps. The threaded ports were hand drilled to permit fluid flow behind the vane in its maximum positions. The complete actuator assembly weighs only 2.4. oz. A mounting tab is included on the actuator body to permit installation of the actuators at the control surface hinge lines.

Breadboard testing and analysis

Moog Series 30 servovalves were selected to permit 10° no-load actuator amplitude up to 25 Hz. The servovalves are flow rated at 1.7 $in.^3$/sec at 1000 psi supply pressure. Port blocks were machined from 2024-T4 aluminum to accept standard 1/4-in. hydraulic tube fittings.

A baseline system with about 19 in. of tubing separating the servovalve and actuator was assembled with the model trailing edge control surface for laboratory testing (Fig. 14). Servoamplifiers were assembled using standard 741 operational amplifiers to provide coil current as a constant function of the input voltage from an EAI TR-48 analog computer which was used to form feedback loops. Actuator shaft angular position was obtained with a small d.c. servo potentiometer.

During testing, the baseline system was unstable at nominal position feedback gains. The system with the surface removed was stable, exhibiting a dominant second-order mode with about 0.3 damping at 99 Hz undamped natural frequency. A linearized approximate mathematical model was derived using the experimental data, Moog servovalve specification data and the simplified system sketch shown in Fig. 15. The dominant second-order mode obtained with the surface removed was included as an equivalent actuator-hydraulic fluid mode.

The derived equations were used in a root locus analysis to qualitatively predict feedback compensation, in addition to position feedback, required for stability. The analysis results indicated shaft angular rate or load pressure with washout feedback provided the required performance at a position loop gain for the desired bandpass. Load pressure feedback was chosen since a miniature rotary tachometer was not available. Load pressure feedback stabilizes the equivalent actuator-hydraulic fluid model, but decreases damping on the servovalve mode. These predicted trends were verified during subsequent baseline system tests. A functional block diagram of the final configuration is shown in Fig. 16.

Angular position transducer

Standard d.c. servo potentiometers could not be used as angular position sensors because of the limited airfoil thickness at the actuator shafts. Position transducers were

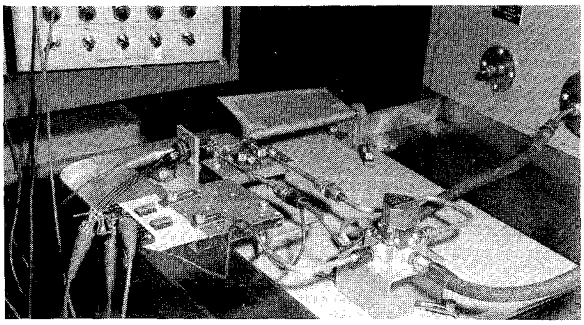

Fig. 14 Wing model baseline actuation system.

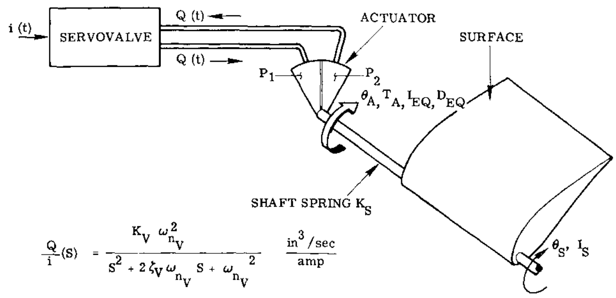

$$\frac{Q}{i}(S) = \frac{K_V\,\omega_{n_V}^2}{S^2 + 2\zeta_V\omega_{n_V} S + \omega_{n_V}^2} \quad \frac{in^3/sec}{amp}$$

$$\frac{\theta_A}{Q}(S) = \frac{\frac{2\beta C_A}{VI_{EQ}}\left(S^2 + \frac{K_S}{I_S}\right)(57.3)\left(\frac{DEG}{IN^3/SEC}\right)}{S\left[\left(S^2 + \frac{D_{EQ}}{I_{EQ}}S + \frac{2\beta C_A^2}{VI_{EQ}} + \frac{K_S}{I_{EQ}}\right)\left(S^2 + \frac{K_S}{I_S}\right) - \frac{K_S^2}{I_{EQ}I_S}\right]}$$

Fig. 15 Sketch of baseline actuation system.

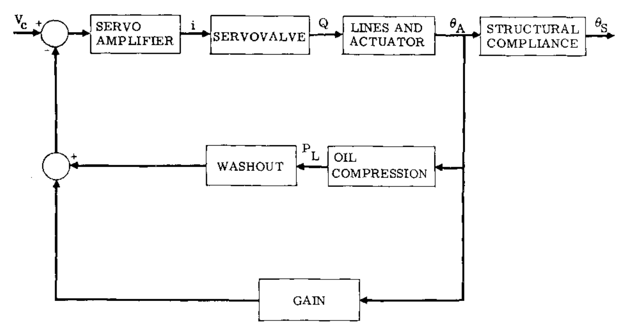

Fig. 16 Functional block diagram of wing model actuation systems.

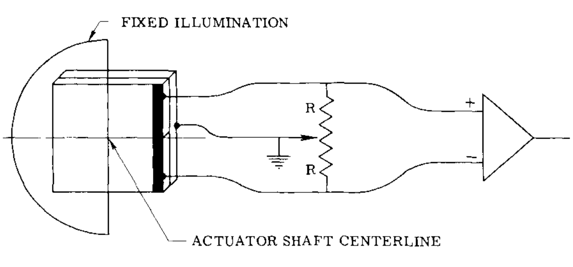

Fig. 17 Angular position transducer.

designed and fabricated using two 0.5 x 0.25 cm silicon solar cells mounted on a common brass base with 0.010 in. gap between the cells as shown in Fig. 17.

The cells are mounted on the actuator shaft with a stationary illumination focused on the cells such that in the null position equal light intensity falls on each cell producing zero potential differential. As the cell assembly rotates with the actuator shaft, the voltage potential differential is proportional to the tangent of the rotation angle. With correct cell loading resistance, provided by an external trim potentiometer, good linearity is attained but the low gradient

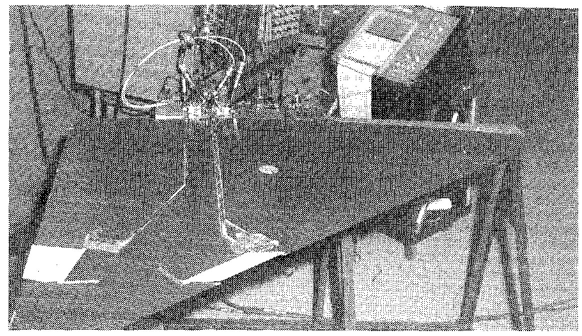

Fig. 18 Wing model with actuation systems installed.

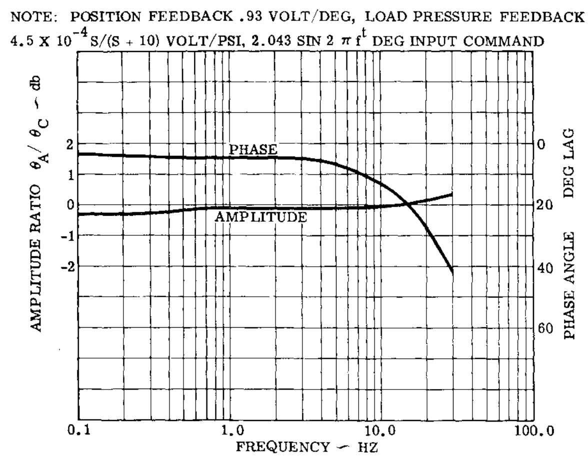

Fig. 19 Wing model leading edge surface actuation system frequency response.

requires amplification of about 400 v/v. Good results have been attained with the transducers during recent wind tunnel tests.

Model Modifications

Figure 18 shows the wing model with the actuation systems installed. The servovalves mount under the fuselage fairing, near the wind tunnel test section wall. Strain gage type pressure transducers are installed on the back side of tee-fittings at the servovalve control ports. The 45 in. of stainless steel hydraulic tubing between the servovalves and actuators consists of 12 in. of 1/4-in. tubing and the remainder 1/8-in. tubing.

The two actuators are cantilevered off the wing structural plate and provide the inboard support for the control surfaces. The d.c. instrument lamps used to provide illumination for the solar cell angular position transducers are supported in brackets mounted on the actuators. The troughs cut in the balsawood for the hydraulic tubing and electrical wires, and the actuator areas were covered and smoothed before recent wind tunnel tests.

A frequency response of the leading edge actuation system obtained just before the wind tunnel entry is shown in Fig. 19. The phase lag at 12 Hz is about 15° and the amplitude variation in the 5 to 25 Hz range is only 0.36 db. Hysteresis measured at the actuator shaft was about ± 0.08°, when the actuator was new.

Phase lag at 12 Hz for the trailing edge actuation system was about 17°, with about 1.9 db amplitude variation in the primary frequency band. Inertia of the trailing edge surface is more than twice that of the leading edge surface. Hysteresis of this system measured about ± 0.06° with actuator broken in to reduce friction between the vane and actuator body and end caps. Performance of both systems has been completely satisfactory in the wind tunnel testing. There has been no sign of hydraulic fluid leakage which could contaminate the 95% freon gas used during the wind tunnel test.

Conclusions

Electromechanical systems can be used in aeroelastic models with the weight and space required for the torque motors, potentiometers, tachometers, and mechanical linkage. Reasonable torque and frequency response are possible although there is a possibility of a shaft torsional mode within the primary frequency range if a long shaft run is required between motor and control surface. A primary advantage is that only electrical wiring is required between the model and tunnel control room.

Electrohydraulic actuation systems can be designed to meet stringent performance, weight, and space requirements. The hydraulic actuator used in this study has over a 200:1 torque/weight advantage over the d.c. torque motor. Because of its small size the hydraulic actuator can be located adjacent to the control surface, thereby eliminating problems caused by shafting torsional characteristics. Hydraulic line dynamics can create a similar type problem although additional feedback compensation can minimize its effects on system performance. The major disadvantage of model hydraulic systems is the need for a hydraulic power supply because testing of models with active control systems usually requires the model to be "free flown" in the tunnel on a cable mount or similar mount system. A miniaturized hydraulic power system, or possibly a small accumulator which could be precharged between tests, is needed to minimize the effect of pressurized hydraulic lines on model dynamics.

References

[1] Redd, L. T., Gilman, J., Jr., Cooley, D. E., and Sevart, F. D., "A Wind-Tunnel Investigation of a B-52 Model Flutter Suppression System," AIAA Paper 74-401, Las Vegas, Nev., 1974.

[2] Sandford, M. C., Abel, I., and Gray, D. L., "A Transonic Study of Active Flutter Suppression Based on an Aerodynamic Energy Concept," AIAA Paper 74-403, Las Vegas, Nev., 1974.